3-9-2017

Effect of Dual Ion Beam Irradiation (Helium and Deuterium) on Tungsten–Tantalum Alloys Under Fusion Relevant Conditions

Sean Gonderman
Purdue University, sean14@purdue.edu

J K. Tripathi
Purdue University

T J. Novakowski
Purdue University

T Sizyuk
Purdue University

A Hassanein
Purdue University

Recommended Citation

Gonderman, Sean & Tripathi, Jitendra & Novakowski, T.J. & Sizyuk, T. & Hassanein, A.. (2017). Effect of dual ion beam irradiation (helium and deuterium) on tungsten–tantalum alloys under fusion relevant conditions. Nuclear Materials and Energy. 12. 10.1016/j.nme.2017.02.011.

Nuclear Materials and Energy 12 (2017) 346–352

Contents lists available at ScienceDirect

Nuclear Materials and Energy

journal homepage: www.elsevier.com/locate/nme

Effect of dual ion beam irradiation (helium and deuterium) on tungsten–tantalum alloys under fusion relevant conditions

S. Gonderman*, J.K. Tripathi, T.J. Novakowski, T. Sizyuk, A. Hassanein

Center for materials under extreme environment (CMUXE), School of Nuclear Engineering Purdue University, West Lafayette, IN 47907, USA

ARTICLE INFO

Article history:
Received 13 July 2016
Revised 3 February 2017
Accepted 14 February 2017
Available online 9 March 2017

Keywords:
Plasma facing materials
Tungsten
Tungsten–tantalum alloy
Helium ion irradiation
Dual ion beam
Surface morphology
Fuzz w layer

ABSTRACT

The selection of tungsten (W) as a divertor material in ITER is based on its high melting point, low erosion, and strong mechanical properties. However, continued investigation has shown W to undergo severe morphology changes in fusion-like conditions. Recent literature suggests alloying W with other ductile refractory metals, *viz.* tantalum (Ta) may resolve some of these issues. These results provide further motivation for investigating W–Ta alloys as a plasma-facing component (PFC) for ITER and future DEMO reactors. Specifically, how these alloy materials respond to simultaneous He^+ and D^+ ion irradiation, and what is the effect on the surface morphology when exposed to fusion relevant conditions. In the present study, the surface morphology changes are investigated in several W–Ta targets (pure W, W-1%Ta, W-3%Ta, and W-5% Ta) due to simultaneous He^+ and D^+ ion irradiations. This comprehensive work allows for deeper understanding of the synergistic effects induced by dual ion irradiation on W and W–Ta alloy surface morphology. Pure W and W–Ta alloys were irradiated simultaneously by 100 eV He^+ and/or D^+ ions at various mixture ratios (100% He^+, 60% D^+ + 40% He^+, 90% D^+ + 10% He^+ ions and 100% D^+ ions), having a total constant He fluence of 6×10^{24} ion m^{-2}, and at a target temperature of 1223 K. This work shows that slight changes in materials composition and He/D content have significant impact on surface morphology evolution and performance. While both the pure W and W–Ta alloys exhibit very damaged surfaces under the He^+ only irradiations, there is a clear suppression of the surface morphology evolution as the ratio of D^+/He^+ ions is increased.

1. Introduction

The magnetic confinement fusion project ITER is leading the way for fusion as future commercial energy source. With the decision to move to a full-tungsten (W) divertor in ITER, the study of W as plasma facing components (PFCs) under fusion environments has become a key issue for the fusion community [1]. W has mainly been selected for its desirable thermo-mechanical properties such as high melting temperature [2], good thermal conductivity [3], and low erosion under ion bombardment [2]. Despite these excellent advantages, recent studies have shown W to undergo severe morphology evolution in response to both low-energy helium (He) and deuterium (D) ion irradiations. W surfaces exhibit blistering after low-energy deuterium irradiation at surface temperatures under 700 K [4–6], and blisters [7,8], pores [9,10], and eventually 'fuzz' [11–14] after low energy helium ion irradiation at surface temperatures between 800 and 2000 K. This surface evolution has been shown to degrade key PFC attributes such as thermal conductivity [15,16] and erosion rate [13,17,18], and these adverse effects have driven research into innovative alternative PFC materials which are resistant to extreme surface modification under relevant fusion conditions.

One area that has shown some promising PFC enhancements is the formation of W alloys. The alloying of W with certain materials like Rhenium (*Re*) has been shown to improve ductility [19,20]. Recently, it has been suggested that although the alloying of W with tantalum (Ta) does not provide the same ductility enhancement as that of the *Re* case; it prevented the crack propagation under certain grain orientations [21]. This result is supported by further research on W–Ta alloy's response to thermal shock via transient heat loading which has shown a significant improvement when compared to pure W materials [21,22]. Along with mechanical enhancements, W–Ta alloys have exhibited a significant reduction in retention of hydrogen (H) isotopes [23–25], as well as a significant resistance to morphology evolution [26].

* Corresponding author.
E-mail addresses: sean14@purdue.edu, sgonderman14@gmail.com (S. Gonderman).

http://dx.doi.org/10.1016/j.nme.2017.02.011

There has been significant work done towards understanding how W responds to low energy He^+ ion irradiation. Previous work showed also the effect of pre-irradiation or sequenced He^+ and D^+ irradiation of materials on their properties such as deuterium retention [27]. However, in a real fusion environment PFC materials will be subjected to dual He^+ and D^+ ion bombardment simultaneously. There have been a few studies looking at the effect of mixed plasmas, but their focus has been mainly on D retention. Studies were performed on W exposed to "D + He" mixture plasma with various He concentrations to investigate the impact on D retention [28,29]. The results suggest that He competes with D for the near surface trapping sites creating deep networks of bubbles in nanometer scale range. These bubbles then act as a diffusion path to the surface for implanted D thus significantly reducing the D retention. Similar work has also been done on the effect of mixed species on surface morphology and D retention [30,31]. This work and studies discussed earlier [29,30] showed similar results demonstrating a significant reduction in D retention due to mixed plasma species effects. It was shown also that surface morphology evolution appeared to be slower as a result of the mixed plasma irradiations [31]. However, this effect was attributed to a dilution of the He flux rather than a mixed plasma effect [31].

The goal of the present work is to focus on the understanding of the morphology responses when both pure W and W–Ta alloys are exposed to simultaneous He^+ and D^+ ion irradiation at elevated temperatures. By changing the mixture ratio of the irradiation species (He^+ and D^+ ions) the synergistic effects of dual ion irradiations are investigated. SEM imaging of ion-exposed samples reveal that He induced microstructures are suppressed due to the presence D, and that the magnitude of this suppression is dependent on the D^+/He^+ ion ratio and the Ta concentration. These results suggest that W based PFCs may respond differently to the fusion environment than previously expected when synergistic effects are taken into account.

2. Experimental methods

The experimental work discussed here studied four different W-based materials, 99.95% pure W and three W–Ta alloys with 1, 3, and 5 wt% of Ta. The 2 mm thick sheets of the W–Ta alloys were sintered at 1500 °C and both the W and Ta powder had an average particle size (APS) of less than 10 μm. When referring to these samples going forward the following name convention will be used: W, W-1Ta, W-3Ta, and W-5Ta will denote the pure W and the 1, 3, and 5 wt% of Ta, respectively.

Samples of the W, W-1Ta, W-3Ta, and W-5Ta were cut from the same sheets into 10 mm × 10 mm × 2 mm samples. A total of 16 W and W–Ta samples were mechanically polished to a mirror finish prior to irradiation. He^+ and D^+ ion exposures were conducted at the UHFI-II chamber located in CMUXE lab at Purdue University [32]. Fig. 1 shows a schematic illustration of the experimental setup used during the irradiation experiments. Four combinations of "He^+ and D^+ ion mixtures" have been used for all the W–Ta samples; He^+: D^+:: 100: 0 (hereafter pure He^+ ion), He^+: D^+:: 40:60 (hereafter 60% D^+ ion), He^+: D^+:: 10:90 (hereafter 90% D^+ ion) and He^+: D^+:: 0:100 (hereafter pure D^+ ion). Note, in an ideal case, the He flux would remain constant for all the mixtures and only adjustment to the D^+ flux would be needed to achieve the necessary ratios. However, the upper limit on the achievable flux for D^+ proved to be 1.4×10^{21} ions m^{-2}-s^{-1}. This means that the He^+ flux at the surface needed to be suppressed to 1.5×10^{20} ions m^{-2}-s^{-1} in order to get the 10:90 He^+-D^+ ratio, and the same fluence and flux for He is used in order to isolate the effect of D on the damage process.

Specifically, 100 eV He^+ ion flux of 4.0×10^{20} ions m^{-2}-s^{-1} at 1223 K, for 4.17 h was used for the experiments with pure He^+ and 60% D^+ ion beams. The He^+ flux was reduced to 1.4×10^{20} ions m^{-2}-s^{-1}, for the experiments with 90% D^+ ion beams, and the irradiation time was increased to get the same total He^+ fluence. The experiments with pure 100 eV D^+ ion irradiation used flux of 6.0×10^{20} ions m^{-2}-s^{-1} at 1223 K, for 4.17 h. Table 1 shows the flux and fluences for each mixture case. After ion irradiation experiments, the samples were taken out from the UHV chamber.

Following irradiation, field emission (FE) scanning electron microscopy (SEM) was performed to monitor the He^+ ion-induced surface modifications. Optical reflectivity measurements were performed over spectra of incident light (using a combination of halogen and deuterium light source and a beam diameter of ~1 mm) ranging from 200 to 1100 nm wavelengths. Before the reflectivity measurements began, the spectrometer was calibrated with a reference plate having 100% reflectivity. Note, the observed reflection in our optical reflectivity system is mainly specular. A specular reflection is a reflection of a mirror-like surface (keeping in mind that different surfaces to different wavelengths may or may not be mirror-like). Specular reflection will result when the surface roughness is smaller than the applied wavelength of light (and diffuse reflection will result when the surface roughness is larger than the wavelength). A specular reflectance of 100% would correspond to an ideal mirror; typical specular reflectance is less than the maximum value. For collecting the reflected light, a "*reflection probe*" has been used which can collect light at the same angle as it illuminates, and can be used for either specular or diffuse reflection measurements. The "*reflection-probe*" is made of 6 illumination fibers around a single read fiber (in the center), which results in a 25° full angle field of view. Each illumination fiber project a cone of light from the source and all of them overlap at the sample in the center, exactly where the central read fiber is situated. Thus, in principle the reflectivity for this ideal mirror will be ~100%. During our measurements the "*reflection probe*" was placed at 90° to the sample surface (along the sample surface normal). The distance between sample and "*reflection probe*" was ~1 mm.

3. Results and discussion

3.1. Field emission scanning electron microscopy (FE-SEM) studies

Fig. 2 depicts the FE-SEM images of 4 W–Ta samples exposed to 100 eV He^+ irradiation only, These ion-exposures represent the base case (reference) for He^+ induced damage; the subsequent mixed ion-species exposures will be compared with these samples. As seen in the four FE-SEM images there is a noticeable morphology difference that is dependent on the Ta concentration. These results are in good agreement with the results observed by our group very recently [27], where we have shown that the alloying of W with Ta alters the crystallographic structure of W causing it to have slightly larger lattice parameter spacing. It appears that the extra lattice spacing provides more available room for the He accumulation before surface damage is observed (in other word, effectively delaying the fuzz morphology evolution of the surface) [27]. This trend is consistent with the FE-SEM images in Fig. 2 where the surface modification is most extreme for pure W and least extreme for W-5Ta.

Fig. 3 shows the FE-SEM images of W–Ta samples irradiated using 100 eV, dual ion (D^+ and He^+) beams, having ion fluxes of 6.0×10^{20} and 4.0×10^{20} ions m^{-2} s^{-1}, for D^+ and He^+ respectively. The images show that the addition of the D^+ flux leads to significant differences in the resulting morphology. First, for the pure W case, the SEM images exhibit a rough porous surface. This contrasts heavily with the tendril, fuzz-like surface as seen in Fig. 2. Second, the W–Ta alloy samples not only show reduced surface damage, but also the appearance of grain boundaries. This is especially clear in the W-3Ta and W-5Ta case. It appears that the

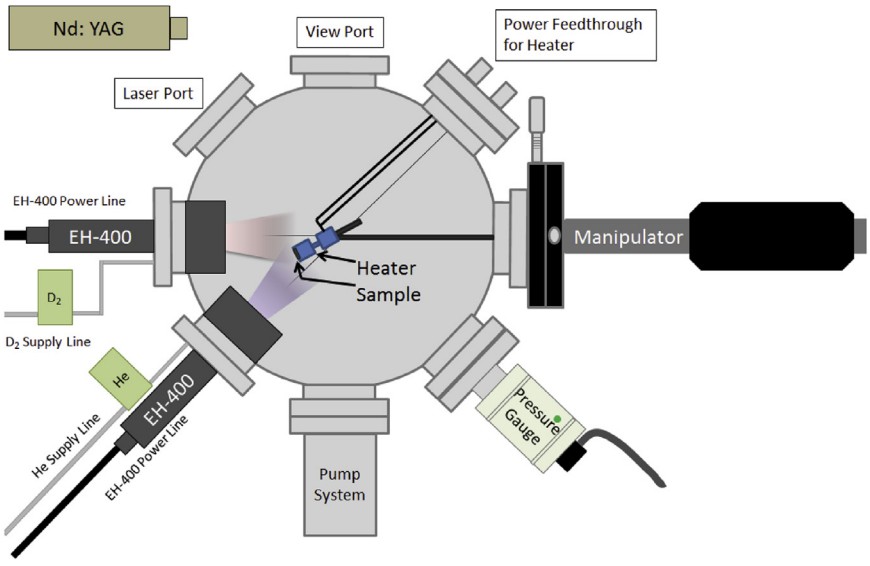

Fig. 1. Schematic diagram of the experimental set up used in UHFI-II for all the ion irradiation experiments.

Table 1
Details of the ion irradiation conditions for the 4 different experiments.

Mixture ratio	He^+ Flux (ions m^{-2} s^{-1})	D^+ Flux (ions $m^{-2}s^{-1}$)	He^+ Fluence (ions m^{-2})	D^+ Fluence (ions m^{-2})	Total Fluence (ions m^{-2})	Irradiation time (hours)
100 He - 0 D	4.0E+20	0	6.0E+24	0	6.0E+24	4.17
40 He - 60 D	4.0E+20	6.0E+20	6.0E+24	9.0E+24	1.5E+25	4.17
10 He - 90 D	1.4E+20	1.4E+21	6.0E+24	6.0E+25	6.6E+25	11.9
0 He - 100 D	0	6.0E+20	0	9.0E+24	9.0E+24	4.17

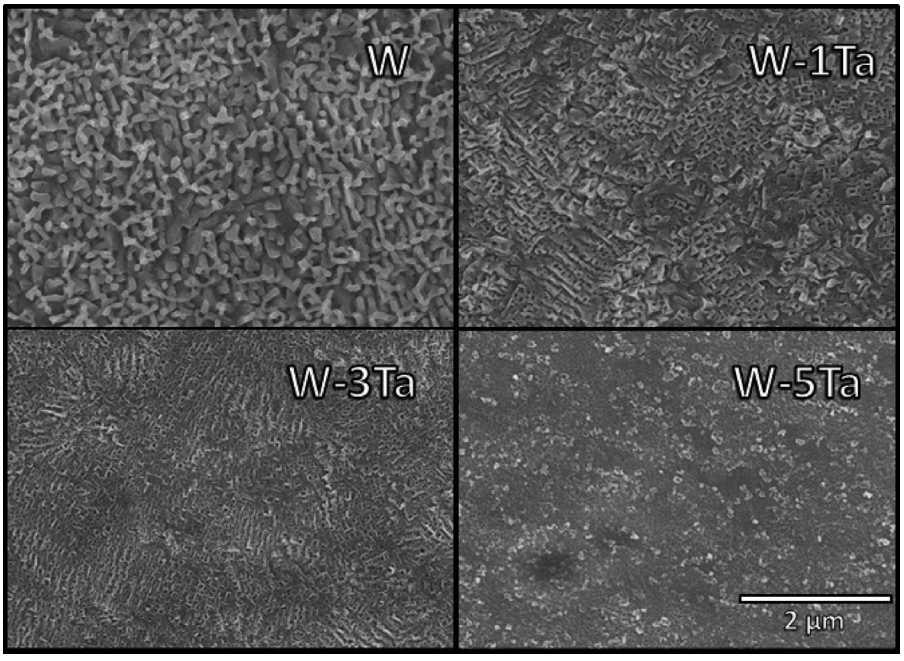

Fig. 2. SEM images of 4 W–Ta samples (W, W-1Ta, W-3Ta, and W-5Ta). Each sample were exposed to 100 eV He^+ irradiation, with a He^+ flux of 4.0×10^{20} ions m^{-2} $s^{-1,}$ for 4.17 h at 1223 K.

W-1Ta case is the transition phase from a porous surface as seen in the pure W case and relatively undamaged surface, showing the appearance of grain boundaries observed in the W-3Ta and W-5Ta cases. The above comparative analysis shows that mixed ion-species are having a significant effect on the modified W surface. The observed findings are in contrast with previous mixed plasma studies [31] which suggested that mixed ion species do not have significant effect on the He induced morphology evolution.

Fig. 4 depicts the FE-SEM images of W–Ta samples which were ion-exposed using 100 eV, dual ion (D^+ and He^+) beams, having ion fluxes of 1.4×10^{21} and 1.4×10^{20} ions m^{-2} s^{-1}, for D^+ and He^+ ions. For this case of lower He^+ concentration the resulting modification on the surface morphology is significantly more pro-

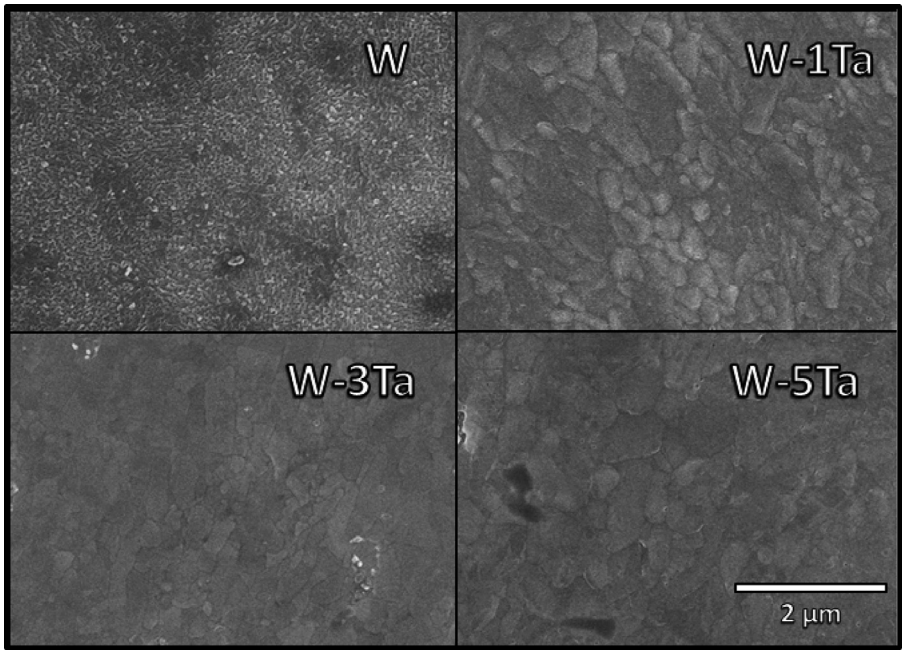

Fig. 3. SEM images of 4 W–Ta samples (W, W-1Ta, W-3Ta, and W-5Ta). Each sample were exposed to 100 eV, D^+ and He^+ irradiation, with a D^+ flux of 6.0×10^{20} ions m^{-2} s^{-1} and a He^+ flux of 4.0×10^{20} ions m^{-2} $s^{-1,}$ for 4.17 h at 1223 K.

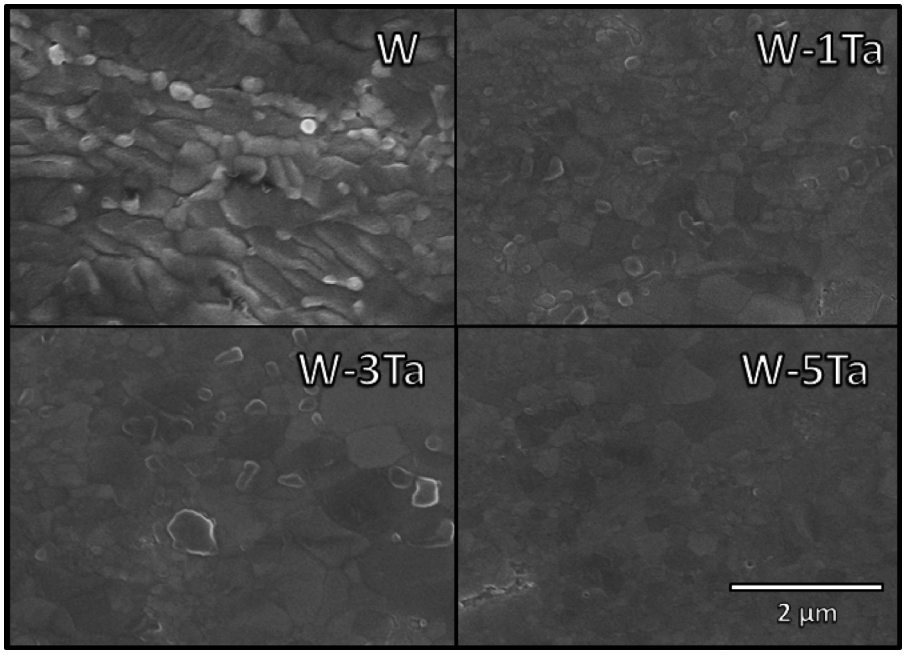

Fig. 4. SEM images of 4 W–Ta samples (W, W-1Ta, W-3Ta, and W-5Ta). Each sample were exposed to 100 eV, D^+ and He^+ irradiation, with a D^+ flux of 1.4×10^{21} ions $m^{-2}s^{-1}$ and a He^+ flux of 1.4×10^{20} ions m^{-2} $s^{-1,}$ for 11.90 h at 1223 K.

nounced. Almost none of the porosity observed previously remains but higher surface roughness is clearly visible (Fig. 4). The "grain boundary" appearance can also be seen clearly even for pure W case (as already observed previously in Fig. 3). Furthermore, the W–Ta samples show a smoother grain boundary surface (Fig. 4). In summary, for 90% D^+ ions and 10% He^+ ions ratio almost all the expected He induced morphology disappeared.

Fig. 5 includes the results of pure D^+ ion beam irradiation of W–Ta samples. All samples show the smooth undamaged surface with the presence of the grain boundaries. As seen in Figs. 3 and 4 the surface evolution trends towards the morphology observed in the pure D^+ exposure. As the ratio of D^+ to He^+ is increased the competition between He and D to occupy the near surface trapping sites will favor the D. This would result in a surface that exhibits damage similar to that of the pure D^+ exposures.

It is known that tungsten exposed to D^+ irradiation above ~ 700 K do not exhibit blistering [4,33]. However, work presented earlier observed a similar recrystallization effect on the surface in response to D^+ only exposures on W at 1473 K [34]. They attributes the observed recrystallization to the fact that the exposures are conducted very near to the recrystallization threshold for W. However, the samples presented in Figs. 3–5 were exposed to D^+ ions at surface temperatures 250 K less than the W samples discussed in [34], and yet a similar recrystallization phenomena is observed.

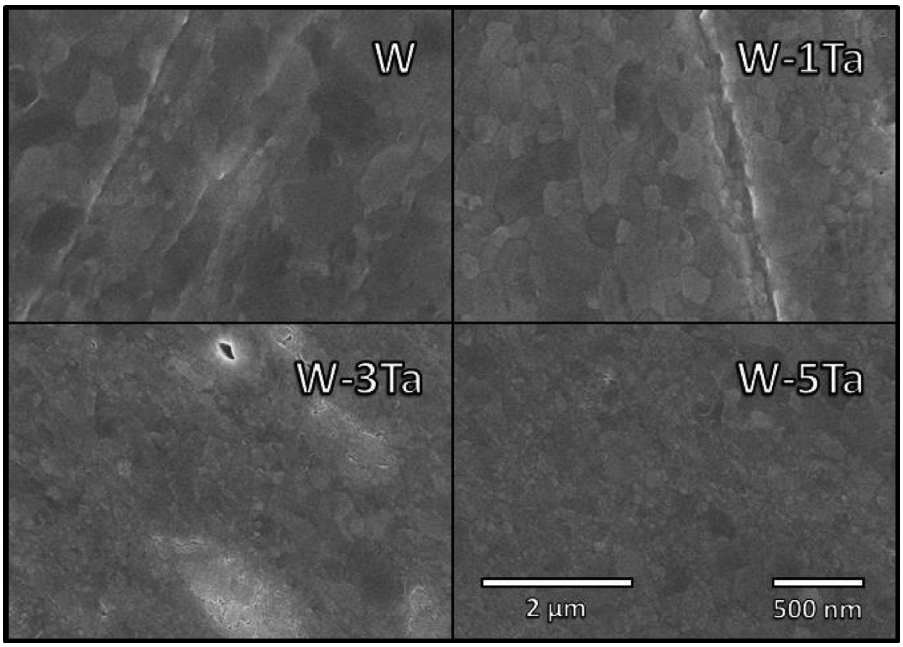

Fig. 5. SEM images of 4 W–Ta samples (W, W-1Ta, W-3Ta, and W-5Ta). Each sample was exposed to 100 eV, D^+ irradiation, with a D^+ flux of 6.0×10^{20} ions m^{-2}-s^{-1}, for 4.17 h at a temperature of 1223 K.

One possible explanation for this observation could be irradiation enhanced recrystallization. Since the surface temperatures of the samples are already near the recrystallization temperature, the addition of ion irradiation can enhance the nucleation rate, increasing crystallization kinetics and effectively reducing the recrystallization temperature of the material [35,36]. This could result in a recrystallizing surface, which does not exhibit significant He induced morphology evolution due to the annealing of defects as a result of the recrystallization process.

One other theory that may explain the grain boundary-like microstructure in both the mixed species and D^+ only exposures is the formation of a W hydride phase on the surface. A similar effect was also discussed in which mixed plasma (D_2-Be-He) exposures resulted in a W-Be phase on the surface which was resistant to He induced structure formation [31]. However, whether or not the grain boundaries observed in Figs. 3–5 are due to some phase formation on the surface remains unclear. There was no other impurity in the plasma like Be which was suggested to be key in the observed structure suppression discussed previously [31].

The results from the FE-SEM images suggest that there is a significant synergistic effect on the surface morphology evolution due to dual D^+ and He^+ irradiation of pure W and W–Ta alloys at high temperatures. In addition to the noticeable difference in surface morphology due to the presence of D, Ta concentration is observed to have an effect on the magnitude of this effect as well. It is possible that irradiation enhanced recrystallization or hydride phase formation at the surface may be the cause of the grain boundary structure observed.

3.2. Optical reflectivity studies

In addition to SEM, optical reflectivity (OR) analysis was also performed to provide a more qualitative analysis of the surface roughness induced by the He^+ and/or D^+ ion-exposures. Fig. 6 shows the optical reflectivity of pristine W, W-1Ta, W-3Ta, and W-5Ta samples prior to irradiation. All the samples show high reflectance prior to irradiation. This is expected as the pre-irradiated samples were all polished to a mirror finish. The pure tungsten sample exhibits slightly higher optical reflectivity, but this is likely due to the quality of the polishing being marginally better. Fig. 7 shows the optical reflectivity plots of irradiated samples after 4 different mixed plasma exposures with varying D^+ ion percent between 0% and 100%. Reflectivity measurements were taken for 700 nm light wavelength. There are several noticeable correlations that can be seen from Fig. 7. First, the total reflectance of the samples increases as the D ion ratio increases. Second, the rate at which the increase in reflectance occurs depends on the Ta concentration in the samples. These trends are the same visual trends observed in the SEM imaging. The SEM images showed a reduction in surface modification as the deuterium ion ratio was increased. This results in a smoother surface and therefore more reflectance. Similarly, the magnitude of the effect of the D^+ ion presence seemed largest in the W–Ta samples. Specially, the W-5Ta and W-3Ta samples showed the smooth grain boundary surface even at the lowest

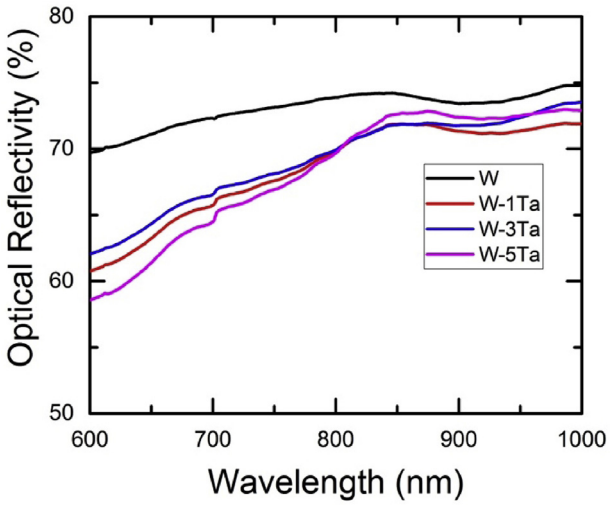

Fig. 6. Plot of the optical reflectivity of pristine W, W-1Ta, W-3Ta, and W-5Ta samples prior to irradiation.

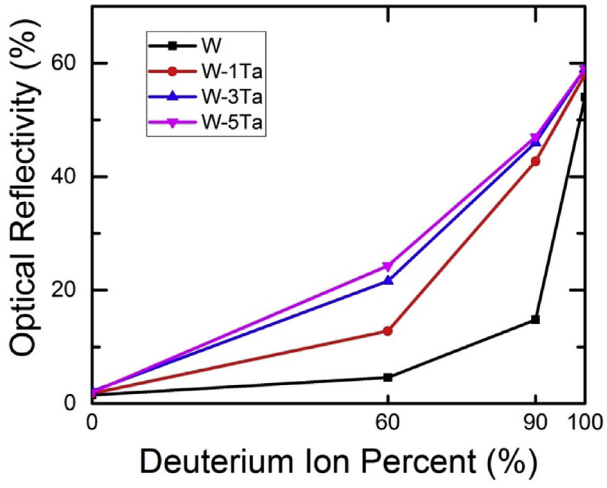

Fig. 7. Plot of the optical reflectivity of irradiated W, W-1Ta, W-3Ta, and W-5Ta samples after 4 different mixed plasma exposures with varying D^+ ion percent between 0% and 100%. Reflectivity measurements were taken for 700 nm wavelength.

D to He ion ratio. This will result in a large increase in reflectance even a low deuterium ion ratios as observed in Fig. 7.

3. Conclusion

The work presented here explores the synergistic effects of dual, He^+ and D^+, low energy ion irradiation of pure W and W–Ta alloys at high temperatures. Post irradiation SEM imaging has revealed an unexpected new microstructure caused by the presence D^+ during the ion exposures. The He^+ only exposure on the W and W–Ta samples yielded the expected surface morphology, but increasing the D^+ ion ratio to 60% and 90% resulted in significant suppression of the He induced damage despite the He flux and fluence remaining the same. The new microstructure appears to be smooth and a covered in grain boundaries. Two preliminary theories have been proposed as explanations for the observed results. First, one possible explanation for this observation could be irradiation enhanced recrystallization. Since the surface temperatures of the samples are already near the recrystallization temperature, the addition of ion irradiation can effectively reduce the recrystallization temperature of the material. This could result in a recrystallizing surface, which does not exhibit significant He induced morphology evolution due to the annealing of defects as a result of the recrystallization process. The second theory that may explain the grain boundary-like microstructure in both the mixed species and D^+ only exposures is the formation of a W hydride phase on the surface.

It is important to note that these observations differ from previously published work which suggest that the presence of D^+ does not have a significant effect on the He^+ induced surface morphology evolution [31]. The cause of this discrepancy remains unclear and requires further investigation. One possible area that may be influencing the observed results is the experimental setup. The experimental set up used in the work presented here utilizes two independent ion sources to control the D^+ ion flux and the He^+ ion flux independently, while the work by Baldwin et al. [31] uses a D_2 - He admixture in the UCSD PISCES-B divertor plasma simulator [37]. Also, the flux of the PISCES-B device is an order of magnitude greater than the ion sources used in the presented work. This allows the work by Baldwin et al. [31] to reach higher irradiation fluences which may explain the difference in the amount of accumulated damage at the surface. It is important to note that the ion fluxes in ITER are expected to be $\sim 10^{23}$–10^{24} ion-m^{-2}-s^{-1} in the divertor region.

These results motivate several important studies that are already underway. First, ongoing analysis such as X-ray photoelectron spectroscopy (XPS) and X-ray diffraction (XRD) are currently being pursued in order to yield information that will suggest if the surface microstructure is being driven by a recrystallization effect or a phase formation on the surface. In conjunction with other post-irradiation analysis, additional experiments are being conducted under different irradiation conditions to help isolate the physical mechanisms driving the different morphologies observed during dual ion beam irradiation of tungsten and W–Ta alloys. Additional experimental work is needed to reconcile the different results obtained on the synergistic effect of multi-ion species irradiation of W materials under relevant fusion conditions presented in [31] and the work presented here.

Acknowledgments

This research was partially supported by National Science Foundation (Grant Number: 1243490-OISE) under the PIRE project.

References

[1] R.A. Pitts, S. Carpentier, F. Escourbiac, T. Hirai, V. Komarov, S. Lisgo, A.S. Kukushkin, A. Loarte, M. Merola, A. Sashala Naik, R. Mitteau, M. Sugihara, B. Bazylev, P.C. Stangeby, J. Nucl. Mater. 438 (2013) S48–S56.
[2] J. Davis, V. Barabash, a. Makhankov, L. Plöchl, K. Slattery, J. Nucl. Mater. 258-263 (1998) 308–312.
[3] P.E.L. Powell, R. W., Cho Yen Ho, National Standard Reference Data System (1966).
[4] K. Tokunaga, M.J. Baldwin, R.P. Doerner, N. Noda, Y. Kubota, N. Yoshida, T. Sogabe, T. Kato, B. Schedler, J. Nucl. Mater. 337-339 (2005) 887–891.
[5] G.N. Luo, W.M. Shu, M. Nishi, J. Nucl. Mater. 347 (2005) 111–117.
[6] W. Wang, J. Roth, S. Lindig, C.H. Wu, J. Nucl. Mater. 299 (2001) 124–131.
[7] S.B. Gilliam, S.M. Gidcumb, N.R. Parikh, D.G. Forsythe, B.K. Patnaik, J.D. Hunn, L.L. Snead, G.P. Lamaze, J. Nucl. Mater. 347 (2005) 289–297.
[8] N. Yoshida, H. Iwakiri, K. Tokunaga, T. Baba, J. Nucl. Mater. 337-339 (2005) 946–950.
[9] S. Sharafat, A. Takahashi, Q. Hu, N.M. Ghoniem, J. Nucl. Mater. 386-388 (2009) 900–903.
[10] S.J. Zenobia, G.L. Kulcinski, Fusion Sci. Technol. 56.1 (2009) 352–360.
[11] M.J. Baldwin, R.P. Doerner, Nucl. Fusion 48 (2008) 035001.
[12] M.J. Baldwin, R.P. Doerner, J. Nucl. Mater. 404 (2010) 165–173.
[13] T.J. Petty, M.J. Baldwin, M.I. Hasan, R.P. Doerner, J.W. Bradley, Nucl. Fusion 55 (2015) 093033.
[14] S. Kajita, W. Sakaguchi, N. Ohno, N. Yoshida, T. Saeki, Nucl. Fusion 49 (2009) 095005.
[15] S. Kajita, S. Takamura, N. Ohno, D. Nishijima, H. Iwakiri, N. Yoshida, Nucl. Fusion 47 (2007) 1358–1366.
[16] D. Nishijima, R.P. Doerner, D. Iwamoto, Y. Kikuchi, M. Miyamoto, M. Nagata, I. Sakuma, K. Shoda, Y. Ueda, J. Nucl. Mater. 434 (2013) 230–234.
[17] M. Tokitani, S. Kajita, S. Masuzaki, Y. Hirahata, N. Ohno, T. Tanabe, Nucl. Fusion 51 (2011) 102001.
[18] Y. Ueda, J.W. Coenen, G. De Temmerman, R.P. Doerner, J. Linke, V. Philipps, E. Tsitrone, Fusion Eng. Des. 89 (2014) 901–906.
[19] P.L. Raffo, J. Less-Common Met. 17 (1969) 133–149.
[20] S. Wurster, B. Gludovatz, R. Pippan, Int. J. Refract. Met. Hard Mater. 28 (2010) 692–697.
[21] M. Wirtz, J. Linke, G. Pintsuk, L. Singheiser, I. Uytdenhouwen, Phys. Scr. T 145 (2011) 014058.
[22] J. Linke, T. Loewenhoff, V. Massaut, G. Pintsuk, G. Ritz, M. Rödig, a. Schmidt, C. Thomser, I. Uytdenhouwen, V. Vasechko, M. Wirtz, Nucl. Fusion 51 (2011) 073017.
[23] Y. Zayachuk, M.H.J. 't Hoen, P.A.Z. van Emmichoven, D. Terentyev, I. Uytdenhouwen, G. van Oost, Y. Zayachuk, Nucl. Fusion 53 (2013).
[24] Y. Zayachuk, M.H.J. 't Hoen, P.a. Zeijlmans van Emmichoven, I. Uytdenhouwen, G. van Oost, Nucl. Fusion 52 (2012) 103021.
[25] Y. Zayachuk, A. Manhard, M.H.J. 'T Hoen, W. Jacob, P.A. Zeijlmans Van Emmichoven, G. Van Oost, J. Nucl. Mater. 464 (2015) 69–72.
[26] S. Gonderman, J.K. Tripathi, T.J. Novakowski, T. Sizyuk, A. Hassanein, Under Prep. (n.d.).
[27] S. Nagata, K. Takahiro, J. Nucl. Mater. 290-293 (2001) 135–139.
[28] M. Miyamoto, D. Nishijima, Y. Ueda, R.P. Doerner, H. Kurishita, M.J. Baldwin, S. Morito, K. Ono, J. Hanna, Nucl. Fusion 49 (2009) 065035.
[29] M. Miyamoto, D. Nishijima, M.J. Baldwin, R.P. Doerner, Y. Ueda, K. Yasunaga, N. Yoshida, K. Ono, J. Nucl. Mater. 415 (2011) S657–S660.
[30] M.J. Baldwin, R.P. Doerner, D. Nishijima, K. Tokunaga, Y. Ueda, J. Nucl. Mater. 390-391 (2009) 886–890.

[31] M.J. Baldwin, R.P. Doerner, W.R. Wampler, D. Nishijima, T. Lynch, M. Miyamoto, Nucl. Fusion 51 (2011) 119501.
[32] J.K. Tripathi, T.J. Novakowski, S. Gonderman, N. Bharadwaj, A. Hassanein, J. Nucl. Mater. 478 (2016) 287–294.
[33] V.K. Alimov, B. Tyburska-Püschel, S. Lindig, Y. Hatano, M. Balden, J. Roth, K. Isobe, M. Matsuyama, T. Yamanishi, J. Nucl. Mater. 420 (2012) 519–524.
[34] B.B. Cipiti, G.L. Kulcinski, J. Nucl. Mater. 347 (2005) 298–306.
[35] J.L. Brimhall, J. Mater. Sci. 19 (1984) 1818–1826.
[36] J.S. Im, H.A. Atwater, Appl. Phys. Lett. 57 (1990) 1766–1768.
[37] Y. Hirooka, J. Vac. Sci. Technol. A Vac. Surf. Film 8 (1990) 1790.